Comparison of Coronal Minimum Intensity Projection CT Reconstructions with Flexible Bronchoscopy for Airway Compression in Children with Lymphobronchial TB

Ahmed Omar Ali Krim

Student number: 475158

Course registered for: MMed (Diagnostic Radiology)

Supervisor: Dr S. Lucas

Prof S. Andronikou

A research report submitted to the Faculty of Health Sciences, University of the Witwatersrand, Johannesburg, in partial fulfillment of the requirements for the degree of Master of Medicine in Diagnostic Radiology

Johannesburg 2017

Declaration

I, Dr Ahmed Omar Ali Krim, declare that this research report is my own work. It is being submitted for the degree of Master of Medicine in the Diagnostic Radiology, at the University of the Witwatersrand, Johannesburg. It has not been submitted before for any degree or examination at this or any other University.

DR AOA KRIM ---------- On this 21 day of December 2017.

Publications and presentations

This work has never been published nor presented at any local or international congresses.

Acknowledgements

I would like to acknowledge the following people; without their help, encouragement and guidance this study would have never been possible.

- My astonishing supervisor, Professor Savvas Andronikou - for his exceptional assistance and endless patience with me, for his continual advice and encouragement, and for his inspiring passion and staunchness for the research. I have learnt so much from him it was truly a privilege to have him as my supervisor.

- My amazing supervisor - Dr. Susan Lucas for her endless assistance, expertise and patience in helping prepare this research report, and for her guidance and support which was much appreciated.

- The co-readers Prof. S Andronikou and Dr. D Bester for spending their valuable time, skills and their expertise in reading the coronal CT MinIP images.

- Prof Victor Mngomezulu for making research a priority in the department.

- Dr. Pierre Goussard and Professor Robert Gie of the Department of Paediatrics, Stellenbosch University for the permission to use their database.

- Noleen Gordon for the data capturing and her unlimited assistance.

- Dr. Alison Bentley for helping with the statistical analysis.

- Finally, and most importantly my wife - Hajir has been extremely supportive of me throughout this entire study and has made countless sacrifices to help me make this a reality. I thank her for her unlimited help, encouragement, and her inspiration in this study - none of this would have been done without her.

Abstract

INTRODUCTION

Tuberculosis (TB) remains one of the most important causes of morbidity and mortality in children in Africa, as well as the rest of the world. Lymphobronchial TB (LBTB) occurs when tuberculous adenopathy affects the airways, either by direct involvement (inflammation and erosion) or by indirect involvement (compression and stenosis). Endobronchial TB (EBTB) is the inflammation of the tracheobronchial tree, which is caused by tuberculosis, and is secondary to the rupture of lymph nodes into the bronchi, or the extension thereof to the peribronchial region, by lymphatic drainage. Identification of airway compromise due to any of these processes can be performed invasively using flexible bronchoscopy or non-invasively with CT scanning, including post processing techniques such as minimum intensity projections (MinIP).

AIM

This retrospective study aimed to generate standardised coronal minimum intensity projection (MinIP) CT reconstructions, and compare these with fibreoptic bronchoscopy in children with LBTB.

METHOD

Standardised coronal MinIP reconstructions were performed from CT scans in children with LBTB and the findings of three readers were compared with flexible bronchoscopy (FB), regarding airway abnormalities. Intraluminal lesions, the site of the stenosis, and the degree of stenosis were evaluated. The length of stenosis was evaluated by CT MinIP only, and no comparison to FB has been made.

RESULTS

65 children with LBTB met the inclusion criteria (38 males; 58.5% and 27 females; 41.5%), with ages ranging from 2.5 to 144 months. Coronal CT MinIP demonstrated a sensitivity of 96% and specificity of 89% against FB. The most common site of stenosis was the bronchus intermedius (91%), followed by the left main bronchus (85%), the right upper lobe bronchus RUL (66%), and

the trachea (60%). Agreement between coronal CT MinIP and FB ranged from 36.9% at the carina to 84.6% at the RLL in normal and abnormal airways.

CONCLUSION

This study has proven that a standardised coronal CT MinIP reconstruction is useful in demonstrating airway stenosis in children with lymphobronchial TB, with sensitivity of up to 96% and specificity up to 89%. The most common sites of stenosis found by the coronal MinIP CT reconstruction were the BI (91%), followed by the LMB (85%), the RUL (66%), and the trachea (60%). The coronal CT MinIP had additional advantages over FB in that it allowed objective measurement of the diameter of the stenosis, measurement of the length of the stenosis as well as visualisation of the post-stenotic segments of the airways. CT MinIP was also able to provide information about lung parenchymal abnormalities.

Standardised coronal MinIP reconstructions are easily performed, as described in our paper, and should be provided with each set of cross sectional MDCT images in children with LBTB. This one single image can provide easily appreciable and useful airway information and additional information not available from FB.

Table of contents

List of Figures

List of Tables

1. Introduction

1.1. Rationale

Tuberculosis (TB) still is one of the most important causes of morbidity and mortality in children in Africa as well as the rest of the world. Lymphobronchial TB (LBTB) is when tuberculous adenopathy affects the airways either by compression, erosion or inflammation. Children have soft airways, which are compressible in comparison to adults and this makes them more likely to be affected by the presence of lymphadenopathy. Flexible bronchoscopy (FB) is the gold standard method for assessing airway disease and in particular airway stenosis in neonates and children.

Computed Tomography Minimum intensity projection (MinIP) is an illustration data method that enables depiction of low-density structures e.g. airways in a 2D projection. Radiologists, who have to spend significant amounts of time generating images on a workstation, are the ones who usually create complex reconstructions. More routine types of reconstructions such maximum intensity projections of the circle of Willis vessels and standardised views of the skull for trauma and abnormal head shapes are performed by technicians who generate these in addition to routine axial reconstructions.
This study aims to compare Coronal MinIP CT reconstructions with FB for airway compression in children with LBTB. Standardised MinIP reconstructions of the airway in the coronal plane may prove to be a rapid mechanism for accurate assessment of the paediatric airway from CT data in a view more familiar to clinicians who are used to looking at frontal chest radiographs.

1.2. TB Epidemiology

TB is infection with Mycobacterium tuberculosis. It is most prevalent in developing countries and is increasing as a result of HIV infection, multidrug-resistant (MDR) TB, drug abuse and poverty (1-3). TB is a common cause of acute and chronic pulmonary disease in adults and children, and the second infectious killer in the world (4, 5). The World Health Organization (6) estimated that more than 9 million new cases were diagnosed and about 1.4 million people deaths from TB in 2011; 990 000 among HIV- negative people and 430 000 HIV-associated TB deaths (6).

1.3. TB in children

TB is one of the top 10 causes of mortality in children (5). According to the 2012 WHO report, approximately 490 000 children were diagnosed with TB in 2011, and an estimated 64 000 children died of TB in this time period (6). Estimating the incidence of TB in children is a challenge (5), and confirmation of the diagnosis is difficult. The microbiological diagnosis of TB in children is difficult due to a significant portion of children being smear-negative as adequate sputum specimens are not easy to obtain (7). In non-endemic areas, the triad of known contact with an adult index case, a positive tuberculin skin test (TST), and suggestive signs on chest X-ray (CXR) is used in clinical practice (8) for the diagnosis of TB in children. The progression from infection to disease among infants (age from 0-5 years) is very high (3, 9).

1.4. TB and HIV in children

Co-infection of TB and HIV is a major issue especially in Africa and other endemic regions (1, 5). The incidence of TB in HIV-positive people is very high, more than 20-times higher than people not infected with HIV (1). HIV-positive infants and children born to mothers with HIV have a high risk of infections with TB because their exposure rate to TB is higher (5). They also have a higher risk of developing TB disease (5). It is important to start these children who are infected with HIV on anti-retroviral therapy (ARV) as soon as possible to decrease the morbidity and mortality, and to start isoniazid prophylaxis against TB (2, 4, 5). A study in HIV-infected South African children showed that Highly Active Antiretroviral Therapy (HAART) reduced the incidence of TB (10), and prevent new episodes of TB infection (11). TB remains the commonest cause of death in HIV-positive children (4).

1.5. Diagnosis of pulmonary TB in children

1.5.1. Clinical evaluation

The first step in the diagnosis of TB is the taking of a good history as the clinical presentation could be similar to any other infection while a history of contact with a known or suspected case of active TB may be the defining clue to the diagnosis.

1.5.2. Laboratory and other methods

Tuberculin Skin Test

The tuberculin skin test (TST) is not 100% sensitive or specific, because both the tuberculin skin test and the interferon (gamma) release assay are not able to differentiate the infection from the active disease of *M tuberculosis* (2), however it is still the most commonly used test for establishing the diagnosis of TB in children (7).

Interferon-gamma release assays

Interferon-gamma release assays (IGRAs) have been developed as an alternative immunodiagnostic approach to the TST for detecting *M. tuberculosis* infection (12).
Both the TST and the interferon-γ release assay cannot differentiate between infection with *M. tuberculosis* and active disease (2).

Microscopy and culture

The gold standard for the diagnosis of TB is culture, but this can take 4-6 weeks for the final result (7). Acid-fast stain and microscopic examination of sputum and gastric lavage are essential for TB diagnosis (7), however obtaining an adequate specimen in children is difficult as children with TB rarely produce sputum voluntarily (8). Samples have to be achieved through specific procedures such as gastric aspirates and induced sputa, but the success of these is still inadequate (8).

Advanced Methods

Newer diagnostic methods are available which improve the diagnostic accuracy, for example, DNA probe methods, polymerase chain reaction (PCR), serodiagnostics, and T-cell diagnosis (7), and detection of mycobacterial antigens (lipoarabinomannan with the assay in urine and Antigen MPB64 with immunochromatographic assay) (2).
Gene Xpert MTB/RIF (Mycobacterium Tuberculosis/ Resistance to Rifampacin) test has attracted a lot of recent interest for diagnosing TB and according to Sekadde and colleagues who used it in Ugandan children (13); this test is accurate and should be used when it is available. However, they showed the sensitivity to be only 68.2% while specificity was high in children at 97.2% (13). Nicol et al. also reported a lower sensitivity of MTB/RIF in children when compared to adults, but the sensitivity was twice that of smear microscopy (14).

1.5.3. Imaging studies for the diagnosis of TB

Chest x-ray (CXR)

This is the most widely used diagnostic imaging method for pulmonary tuberculosis. It can also detect pleural effusion, miliary TB, and hilar lymphadenopathy (2). CXR is not very sensitive for detection of lymph nodes and their complications, (airways stenosis or obstruction) but remains a very useful imaging modality in the diagnosis of TB (3).

Computed Tomography (CT)

CT is the most sensitive and specific imaging modality to diagnose primary pulmonary TB and its complications: mediastinal lymphadenopathy, parenchymal changes, pleural /pericardial effusions (15, 16) and extra-pulmonary tuberculosis. It is also the modality of choice in the diagnosis of airways involvement (17, 18). CT will be discussed in more detail in Section 2.7: MDCT of the chest in children.

Magnetic resonance imaging (MRI)

MRI with fast imaging sequences (without contrast administration) has been found very useful to detect chest abnormalities of infection in children when compared to chest radiography and MDCT (19, 20). The features of pulmonary TB can be demonstrated with MRI. Mediastinal and hilar nodes are demonstrated equally well on MRI and CT scan (21). STIR imaging is particularly useful in demonstrating lymphadenopathy as high-signal masses in recognized regions (21, 22) but there is a suggestion that the necrosis particular to TB, occurring centrally in tuberculous lymphadenopathy, may yield a low TS/STIR signal as it has been shown to do in the lung parenchyma (23).

Ultrasound

Ultrasound is useful in detection of abdominal tuberculosis, confirmation of pleural or pericardial effusions as well as detection of lymph nodes and guidance of biopsies (2).

1.6. Lymphobronchial and endobronchial and TB in children

Children with pulmonary TB may have significant airway involvement by lymphadenoathy in 35 to 38% of cases (15, 24). This is demonstrated in a large study from South Africa by Theart et al., where out of the 1277 cases of TB entered into the study, 206 were children with intrathoracic TB. Of these 206, 79 (38.3%) demonstrated complicated lymph node disease (24). Another study from South Africa utilising CT, by Andronikou and colleagues, demonstrated

35/100 (35%) of children with TB had airway compressions (15). Airway involvement by TB as described above in children is referred to as **Lymphobronchial TB (LBTB).** This occurs either by compression, erosion or inflammation (2, 25, 26).

Endobronchial TB (EBTB) is defined as inflammation of the tracheobronchial tree caused by the mycobacterial bacilli (27) and is secondary to rupture of lymph nodes into the bronchi or extension to the peribronchial region by lymphatic drainage (28).

1.6.1. Airway stenosis due to LBTB

Airways obstruction or narrowing in LBTB may be extraluminal or intraluminal.

The extraluminal obstruction is caused by enlarged tuberculous lymph nodes. Although a single group of nodes could be involved, it is much more common for multiple nodal sites to be involved (25, 26). The commonest sites of lymph node involvement are subcarinal and right paratracheal, followed by right hilar and left hilar (3, 15, 21, 26). The commonest and most frequent anatomical sites of airway compression by LBTB are the bronchus intermedius and the left main bronchus (26, 29). Intraluminal airway obstruction occurs by erosion of caseated lymph nodes into airways or intraluminal inflammatory changes (25, 28, 30).

1.6.2. Diagnosis of LBTB

The diagnosis of LBTB hinges on identifying airway involvement by tuberculous lymph nodes. Any of the above imaging modalities can be used to detect airway narrowing, but direct visualisation through flexible bronchoscopy (FB) is considered the gold standard for the diagnosis of airway involvement (31).

1.7. Bronchoscopy in children with LBTB

Flexible bronchoscopy has become a routine investigation in children with complicated pulmonary TB (32). It is used to confirm the TB diagnosis by bronchial lavage and biopsy of lymph nodes as well as to identify the site and degree of airway narrowing or obstruction (32, 33). Flexible bronchoscopy (FB) is the gold standard modality for assessing airway disease and in particular airway stenosis in children and neonatal intensive care (32, 34). FB has the advantage that transbronchial enucleation and aspiration of endobronchial material can be done at the time of the bronchoscope (25).

1.7.1. Problems, limitations and complications of FB

Paediatric FB is an invasive procedure that usually requires general anaesthesia although it can be done under sedation in selected cases. It requires pre-procedural preparation as well as post-procedural monitoring (17, 34).

FB has difficulty in assessing the distal airways when there is severe stenosis more proximally, preventing passage of the bronchoscope. It is also unable to measure the length of stenosis when it is unable to pass an area of narrowing. It has a further limitation in that it is unable to determine the cause of any external compression (31).

The performance of the procedure in children requires training and experience, carries significant costs and has well described associated complications including major complications of apnoea, bradycardia, respiratory depression and oxygen desaturation (more frequent in young children) and minor complications (epistaxis, airways bleeding, excessive cough and laryngospasm) (34).

1.8. Multi-detector CT of the chest in children with LBTB

Multi-detector CT of the chest (MDCT) plays a significant role in patients with airway obstruction in general and more specifically in patients with LBTB (26). MDCT can assess children with signs and symptom of airway obstruction prior to FB with regards to the presence of lymphadenopathy, lung parenchymal changes, pleural disease as well as airway attenuation. The use of a variety of algorithms and reconstruction techniques can enhance these evaluations (2, 18).

1.8.1. Features of LBTB on MDCT

The appearance of the lymph nodes on post contrast CT scan has been described by several authors (9, 15, 26). These changes include rim-enhancement of lymphadenopathy with central low density or more often ‘ghost-like’ enhancement. TB lymphadenopathy can also demonstrate homogenous enhancement. The subcarinal and right paratracheal sites have been shown as the commonest sites for lymphadenopathy (3, 26). The commonest sites of airway compression are the left main bronchus, right main bronchus, the bronchus intermedius and trachea (25, 26).

Other findings of LBTB include lobar collapse, soft tissue masses or granulation tissue within the bronchus with a ball-valve effect (26, 35), as well as intraluminal herniation of caseating lymph

nodes or intraluminal fluid due to bronchial ulceration or the inflammatory process (28, 36, 37). Other associated findings include pleural or pericardial effusion, consolidation, cavitation, and miliary nodules (2, 26).

1.9. MDCT reconstructions and post-processing

The widespread use of MDCT and technological revolutions in imaging post-processing software has yielded a number of widely available techniques which are currently in clinical use: volume rendering (VR) including virtual endoscopy (VE), shaded Surface display (SSD), maximum intensity projections (MIP), and minimum intensity projection (MinIP). These can be employed to add significant value to the diagnostic modalities and are especially useful for demonstrating pathology to clinicians and parents, especially when surgical planning is entertained (38).

2.9.1. MinIP reconstructions

Minimum intensity projection (MinIP) is an illustration data method that uses detection of low-density structures (lowest Hounsfield value) (38, 39) and projecting this in a 2D reconstruction. It is a simple reconstruction technique (40) that is useful for the detection of concentric bronchial stenosis or postoperative extrabronchial air collection (39).

This post processing reconstruction technique is useful to identify airway compression due to LBTB and has the added advantage that it can measure the length of stenosis that is too tight for a bronchoscope to pass through (40). It can also visualize the airways distal to these tight stenoses. Because it is a 2D projection, it is not always accurate to determine 3D relations (39, 40) but the coronal view can provide images easily correlated with plan radiographic frontal projections for clinicians to better appreciate the disease location and severity (40).

1.10. Aim

This retrospective study aims to generate and compare standardised coronal CT MinIP reconstructions of the paediatric airway with fibreoptic bronchoscopy in children with LBTB.

1.11. Study Objectives

1. To develop a standardised protocol for producing standardised coronal CT MinIP reconstructions of the chest for routine airway evaluation in children.

2. To determine feasibility and accuracy of interpretation of standardised routine coronal CT MinIP in paediatric chest TB imaging by:
    (a) Comparing the site of airway compression detected with CT MinIP to FB.
    (b) Comparing the degree of airway narrowing of CT MinIP to FB.
    (c) Comparing the intraluminal lesions detected with CT MinIP to FB
3. Demonstrating the ability to document the length of compression of airway narrowing on CT MinIP.

2. Methods

2.1. Study design

This study was a retrospective descriptive cross-sectional study, using an existing CT scan database of children with LBTB, imaged over a ten-year period. The study was performed in the Radiology Department of the University of the Witwatersrand (WITS), in Johannesburg, South Africa. However, the database was derived from the Tygerberg Hospital Paediatric Pulmonology Department, at the University of Stellenbosch, with permission of the gatekeeper. This study was therefore nested in a larger study of paediatric LBTB.

Ethics clearance for the larger study was obtained from the Stellenbosch University Research Ethics Committee (N10/08/282) and local approval was obtained from the University of the Witwatersrand Human Research Ethics Committee (appendix A clearance certificate M130664).

2.2. Sample

The patients in the larger study included children who had presented with symptoms and signs of airways compression, and who had been treated for respiratory tuberculosis at Tygerberg Hospital — a tertiary care hospital in Cape Town, South Africa. The patients were treated with a month-long anti-TB treatment, to which steroids had been added. If the symptoms persisted, they underwent FB and CT scans as part of their routine management.

Children below 13 years of age (156 months) making up the most recent 100 cases that had received CT scans and FB, formed the available database for this study; however, after the inclusion and exclusion criteria were applied as described below, only 65 cases remained as the study population.

2.2.1. Inclusion criteria

100 most recent sequential children who had undergone CT scans on a 16-slice MDCT (multi-detector computerised tomography) scanner from the available database, were included in this study if they met the following criteria:

- The patients flexible bronchoscopy (FB) results were available in the database;
- Patients were below 13 years of age;
- Patients had undergone high resolution CT scans, consisting of ≥150 images to generate full chest scans; and

- Patients were known to have LBTB (i.e. confirmed TB with airway symptoms).

2.2.2. Exclusion criteria

Patients were excluded from this study if they met the following criteria:

- The patients CT scans contained corrupted data, precluding accurate reconstructions;
- There were significant motion artefacts in the source CT data precluding adequate reconstruction;
- The patients had incomplete bronchoscopic data; or
- The patients were intubated or significantly malpositioned during the scanning procedure which precludes adequate evaluation of the airway.

2.3. Materials and Methods

The original high resolution MDCT data was used for creating the coronal MinIP reconstruction using the OsiriX DICOM Viewer, 32-bit (version 5.6) software. Reconstruction was performed by the primary investigator, who developed a standardised technique on ten pilot patients using the same inclusion and exclusion criteria as the main data set. These patients were not used for generating the final results.

A fixed-slab thickness range from 5 mm to 20 mm was used (only three cases in the main data set could be performed with a thickness less than 10 mm thickness). The selected landmark for coronal oblique angulation was the length of the trachea as seen on the sagittal image. The instructions and reconstruction parameters determined as a guideline for producing standardised images are listed below:

1. The source CT is opened in the MPR application of the OsiriX program, where by the trachea on sagittal plane must be peripendicular to the carina on axial plane, using the vertical and transverse axis, with the midpoint at the Level of the carina.
2. The correction of the orientation of the coronal view is planned by angling the transverse axis along the carina, and by keeping the vertical axis along the trachea on coronal plane reconstruction (Figure 2.1.).

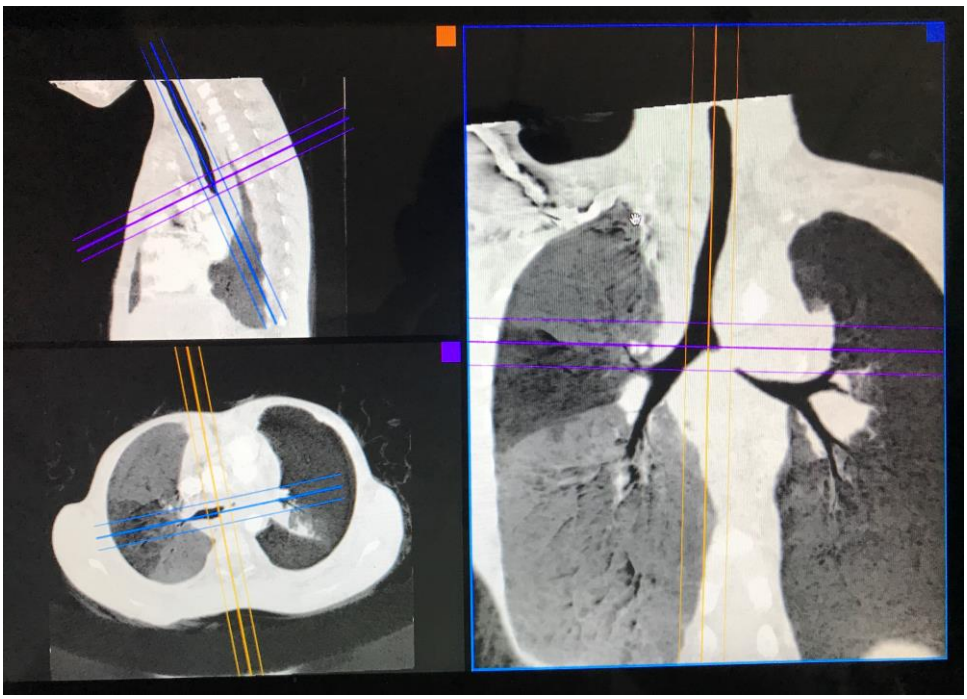

Fig: 2.1: Shows the MPR image with correct axis positioned on saggital and axial planes to produce single coronal image.

3. The viewing window is now set to 'lung window' and the MinIP reconstruction selection is obtained.
4. The acceptable slab thickness of the MinIP reconstruction (range between 5 and 20 mm) is selected to provide complete visualisation of the full antero-posterior thickness of tracheobronchial tree on the single coronal oblique image.
5. Centralisation and zooming of the image can now be performed
6. The single image is now saved as a DICOM-format file in the OsiriX program, and labelled appropriately).

For this study the single standard image from OsiriX platform carrying only basic annotation (no name), using only a study number, and listing the thickness of the slab was exported into a secured file on computer for the readers to interpret on individual computers.

Interpretation /reading of the coronal MinIP slabs was performed by the primary investigator (a senior registrar in radiology the time), one other senior registrar in radiology, and the supervisor (consultant paediatric radiologist with over fifteen-years of experience interpreting paediatric TB radiographs and CT scans). Readers were blinded to each other and to the bronchoscopy findings, and a consensus majority decision was reached for each site of airway

stenosis from the three readings. Any areas of perceived stenosis, as recorded by majority consensus, were used for comparison against FB. Readers also evaluated the degree of obstruction at the ten sites along the tracheobronchial tree, as per the data collection sheet (Appendix B), which matched FB evaluation of the airways (see Appendix C). These sites were the trachea, the carina, the right and left main bronchi, the right upper lobe bronchus, the bronchus intermedius, the right middle lobe bronchus, the right lower lobe bronchus, the left upper lobe bronchus, and the left lower lobe bronchus.

2.4. Calculation of the percentage and grading of obstruction

The decision of the degree of airway stenosis was made by the agreement of at least two of the three readers, and the final stenosed airway measurement was calculated as the average of the readers' measurements who had identified and measured the stenosis.

Numeric measurement data from the most severely-narrowed region of each involved airway segment was acquired and expressed as a percentage, based on a ratio derived in relation to 'normal airway' proximal to the obstruction. The percentage of stenosis was calculated using the following formula:

$$1 - (S/N) \times 100 = \%$$

Where:

S= Stenosis minimum; and

N= Normal measurement above or below the stenosed region.

The grading below was used based on that used during bronchoscopy to facilitate comparison between the two investigations:

- No obstruction 0% - Grade 0;
- Mild obstruction 1-50% - Grade 1;
- Moderate obstruction 51-75% - Grade 2;
- Severe obstruction 76-99% - Grade 3(a);
- Complete obstruction 100% - Grade 3(b);

FB findings were accessed from the notes using same categories of presence and severity of stenosis (as per section 2.3, above). The length of stenosis measured using the coronal CT MinIP was also recorded.

2.5. Data collection

The data was collected according to the attached data collection sheet (see Appendix B) for each reader. The final data, based on the majority decisions, were entered into the Research Electronic Data Capture (REDCap) website using a secured username and password, along with the bronchoscopy data and the patients' details. Then, the data for the coronal CT MinIP reconstruction and FB were exported from the REDCap website onto an Excel spread sheet, for statistical calculation and data analysis.

2.6. Statistical analysis

The findings of the coronal CT MinIP were compared to the FB findings.

Comparative statistics of agreement were calculated, both concerning the presence of stenosis at each site, and concerning the degree of stenosis - the Chi Square test and the Cohen's Kappa test was used in the evaluation by using the STATA data analysis software application.

3.Results

3.1. Demographics

Children evaluated were below 13 years (156 months) of age. Only the most recent 100 adequate cases diagnosed with LBTB who had CT scans and FB results were considered. Of these, 35 cases were excluded.

A total of 65 children with LBTB made up the final study population. This comprised 38 males (58.5%) and 27 females (41.5%), with ages ranging from 2.5 to 144 months, (mean age 23.85 months; median age 14 months). Of these 55 patients (84.6%) were below 40 months of age, and only 5 patients (7.7%) were above 80 months

3.2. Technical report

The 3D MPR application with curved angle technique was used, and the slab thickness of the coronal MinIP for visualizing all ten airways on a single coronal image ranged from 5.95 mm to 20 mm (mean 12.82 mm; StDev: 3.34 mm). Only 3 MinIP images had a thickness below 10 mm (4.6%), while 44 images (67.7%) ranged from 10 mm to 15 mm, and 18 images (27.7%) had a thickness above 15 mm.

3.3. Airway stenosis on coronal CT MinIP reconstruction

3.3.1. Sites of stenosis detected with CT MinIP

Ten airway sites were examined for airway stenosis on the reconstructed CT scans (fig 3.1): trachea, carina, right main bronchus (RMB), bronchus intermedius (BI), right upper lobe bronchus (RUL), right middle lobe bronchus (RML), right lower lobe bronchus (RLL), left main bronchus (LMB), left upper lobe bronchus (LUL), and left lower lobe bronchus (LLL). Airway stenosis was detected in all-65 patients (as expected from the clinical inclusion criteria) with variable degrees and sites of stenosis along the bronchial tree.

Only one patient had a single site affected (LMB), and one patient had two sites affected (trachea and BI). Most of the patients had multiple sites of stenosis, as summarised in Table 3.1. including 2 patients with stenosis at all 10 sites evaluated. The number of stenosed airways for the 65 patients are summarised according to affected site in Table 3.2.

Table 3.1. Number of patients according to number of airway sites demonstrating stenosis on coronal MinIP CT scan reconstructions

No of sites	One site	Two sites	Three sites	Four sites	Five sites	Six sites	Seven sites	Eight sites	Nine sites	Ten sites
No of patients	1	1	12	6	19	6	10	4	4	2

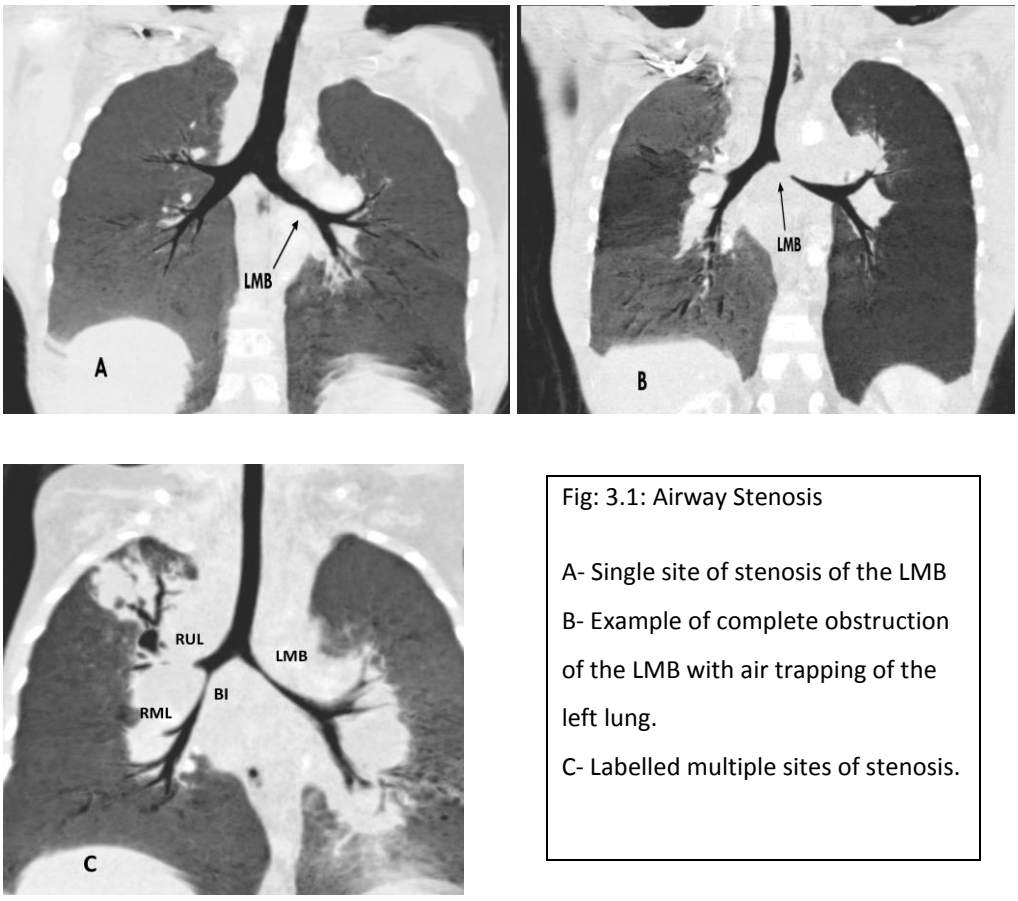

Fig: 3.1: Airway Stenosis

A- Single site of stenosis of the LMB
B- Example of complete obstruction of the LMB with air trapping of the left lung.
C- Labelled multiple sites of stenosis.

Figure 3.1. Examples of single and multiple airway stenoses (A, B, C) on coronal CT MinIP reconstructions

Table 3.2: Number of sites of airway stenoses on coronal MinIP

Airway Site	Trachea	Carina	RMB	RUL	BI	RML	RLL	LMB	LUL	LLL	Total Sites (n=650)
Patients n = 65	39	26	26	43	59	23	11	55	32	38	352
%	60%	40%	40%	66%	91%	35%	17%	85%	49%	58.5%	54%

There were 352 sites of airway stenosis out of a total of 650 possible sites (54%). The commonest site of airway stenosis on the coronal MinIP CT reconstruction was the BI, followed by LMB, RUL, and the trachea.

3.3.2. Intraluminal lesions and length of stenosis measurement on CT MinIP

There were 23 intraluminal lesions found by the coronal CT MinIP - the commonest sites were the BI (8 patients), LMB and LUL (4 patients each site), as shown in more detail in Table 3.3. The ability of CT MinIP to demonstrate the length of stenoses is summarised in Table 3.4 for seven sites while figure 3.2 demonstrates three different patients with measurement of the length of stenosis.

Table 3.3. Intraluminal lesions detected on coronal CT MinIP

	Trachea	Carina	RMB	RUL	BI	RML	RLL	LMB	LUL	LLL	Total
CT MinIP	0	0	2	3	8	0	1	4	4	1	Yes=23

Table 3.4. Length measurement of stenosis on coronal CT MinIP

	Number of cases	Minimum measurement/ mm	Maximum measurement/mm	Mean	STD Dev
Trachea	39	3	50	12.03	8.60
RMB	26	2.7	8	4.98	1.16
RUL	43	2.2	20	5.43	3.15
BI	59	2	19	9.15	4.77
LMB	55	1.5	30	15.83	5.90
LUL	32	2	9	4.76	2.00
LLL	38	2.5	12	5.93	2.49

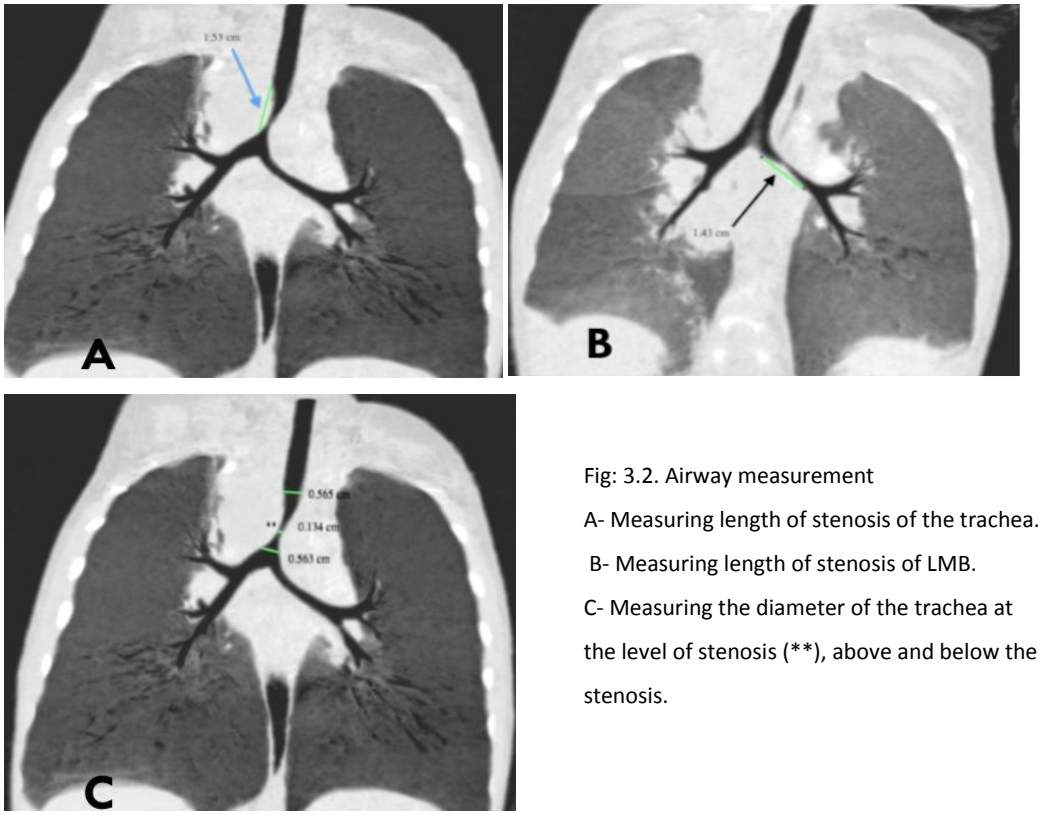

Fig: 3.2. Airway measurement
A- Measuring length of stenosis of the trachea.
B- Measuring length of stenosis of LMB.
C- Measuring the diameter of the trachea at the level of stenosis (**), above and below the stenosis.

Figure 3.2. Examples of airway stenosis with length and thickness measurements in 3 different patients with CT MinIP.

3.3.3. Severity / degree of stenosis detected with coronal MinIP

The severity of the stenosis was classified into five grades as summarised in Table 3.5: Grade 1 to Grade 3b represent an increasing severity/ degree of stenosis of the affected airways on the coronal CT MinIP reconstructions.

Table 3.5: Severity/ degree of stenosis on CT MinIP according to site

Site of the Airway	No of patients	Grade 1	Grade 2	Grade 3a	Grade 3b
Trachea	**39/65 (60%)**	31/39 (79.5%)	4/39 (10.25%)	4/39 (10.25%)	0
Carina	**26/65 (40%)**	25/26 (96%)	1/26 (4%)	0	0
RMB	**26/65 (40%)**	9/26 (34.6%)	12/26 (46.2%)	2/26 (7.7%)	3/26 (11.5%)
RUL	**43/65 (66%)**	7/43 (16.3%)	19/43 (44.2%)	4/43 (9.3%)	13/43 (30.2%)
BI	**59/65 (91%)**	13/59 (22%)	20/59 (34%)	10/59 (17%)	16/59 (27%)
RML	**23/65 (35%)**	0	0	4/23 (17%)	19/23 (83%)
RLL	**11/65 (17%)**	0	3/11 (27.3%)	2/11 (18.2%)	6/11 (54.5%)
LMB	**55/65 (85%)**	3/55 (5.4%)	23/55 (42%)	23/55 (42%)	6/55 (10.6%)
LUL	**32/65 (49%)**	9/32 (28.1%)	14/32 (43.8%)	4/32 (12.5%)	5/32 (15.6%)
LLL	**38/65 (58.5%)**	11/38 (29%)	18/38 (47.3%)	5/38 (13.2%)	4/38 (10.5%)
% Of total patients possible sites	**352/650 54.2%**	**108/650 16.6%**	**114/650 17.4%**	**58/650 9%**	**72/650 11%**
% Of stenoses		**108/352 30.7%**	**114/352 32.4%**	**58/352 16.5%**	**72/352 20.5%**

Keys; Grade 1 = Mild Obstruction 1-50%, Grade2 = Moderate obstruction 51-75%, Grade3a = Severe obstruction 76-99% and Grade3b = Complete obstruction 100%.

3.4. Comparison of coronal MinIP CT reconstruction results with FB data

3.4.1. Site of the stenosis and the degree of the obstruction determined by FB

Both the flexible bronchoscopy and the CT MinIP studies have detected the stenosis in the 65 patients, FB determined that there were 266/650 (41%) sites of stenosis in the 65 patients, considering that each patient had 10 possible sites of stenosis. The severity and sites of the stenosis determined using FB are summarised in Table 3.6.

Table 3.6: Sites of stenosis and the degree of the obstruction using FB

Site of the Airway	Number of sites affected	Grade 1	Grade 2	Grade 3a	Grade 3b
Trachea	**42/65 (64.6%)**	35/42 (83%)	5/42 (12%)	2/42 (5%)	0
Carina	**57/65 (87.69%)**	57/57 (100%)	0	0	0
RMB	**9/65 (13.84%)**	3/9 (33.3%)	0	5/9 (55.6%)	1/9 (11.1%)
RUL	**24/65 (36.9%)**	14/24 (58.2%)	3/24 (12.5%)	2/24 (8.3%)	5/24 (21%)
BI	**49/65 (75.38%)**	12/49 (24.5%)	15/49 (30.6%)	17/49 (34.7%)	5/49 (10.2%)
RML	**19/65 (29.23%)**	11/19 (58%)	2/19 (10.5%)	2/19 (10.5%)	4/19 (21%)
RLL	**7/65 (10.76%)**	7/7 (100%)	0	0	0
LMB	**46/65 (70.76%)**	28/46 (61%)	10/46 (22%)	6/46 (13%)	2/46 (4%)
LUL	**7/65 (10.76%)**	6/7 (86%)	0	0	1/7 (14%)
LLL	**6/65 (9.2%)**	6/6 (100%	0	0	0
Percentage %	**266/650 (41%)**	**179/650 (27.55%)**	**35/650 (5.45%)**	**34/650 (5.22%)**	**18/650 (2.78%)**
Percentage of stenoses		**179/266 (67%)**	**35/266 (13%)**	**34/266 (12.8%)**	**18/266 (6.8%)**

Keys; Grade 1 = Mild Obstruction 1-50%, Grade2 = Moderate obstruction 51-75%, Grade3a = Severe obstruction 76-99% and Grade3b = Complete obstruction 100%.

3.4.2. Comparison of sites of airway stenosis detected by coronal CT MinIP with FB

The total number of airways with stenosis identified on CT MinIP was 352 (54%), and the total number of airways with stenosis determined by FB was 266 (41%). The commonest airway affected with compression and stenosis on the CT MinIP was BI (59/65; 91%), while the commonest airway stenosis determined by FB was the carina (57/65; 88%).

The comparison according to the site is summarised in table 3.7 and figure 3.3 below.

Table 3.7: Comparison of CT MinIP and FB with regard to number of airway stenoses detected according to site

Modality	Trachea	Carina	RMB	RUL	BI	RML	RLL	LMB	LUL	LLL	Total stenoses
MinIP N = 65	39 (60%)	26 (40%)	26 (40%)	43 (66%)	59 (91%)	23 (35%)	11 (17%)	55 (85%)	32 (49%)	38 (58.5%)	352 (54%)
FB N = 65	42 (65%)	57 (88%)	9 (14%)	24 (37%)	49 (75%)	19 (29%)	7 (11%)	46 (71%)	7 (11%)	6 (9%)	266 (41%)

Figure 3.3. Graphs comparing the sites of the airway stenosis of CT MinIP and FB in (a) absolute numbers and (b) percentages

(a)

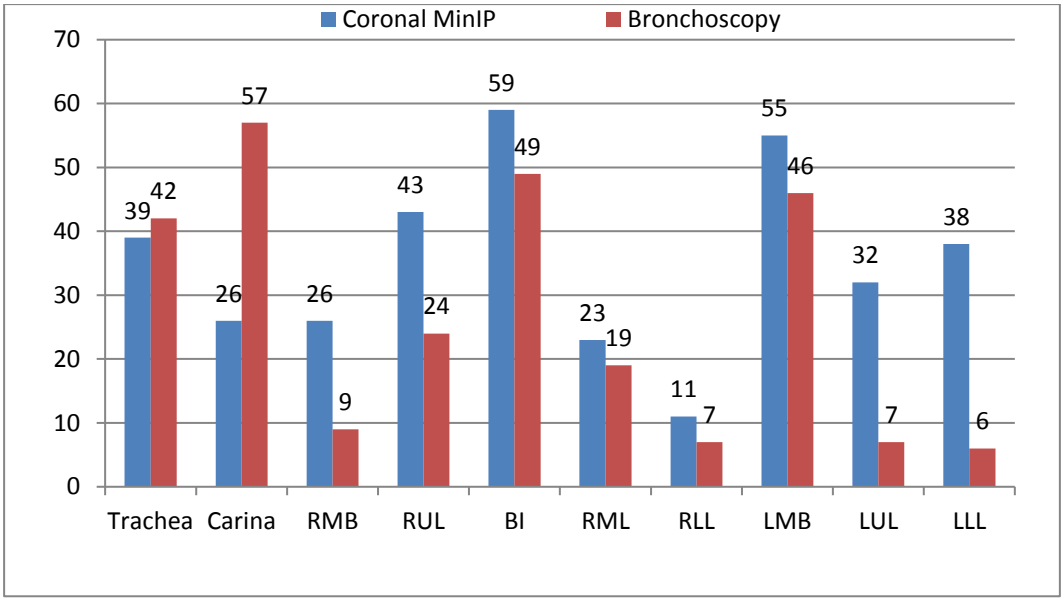

(b)

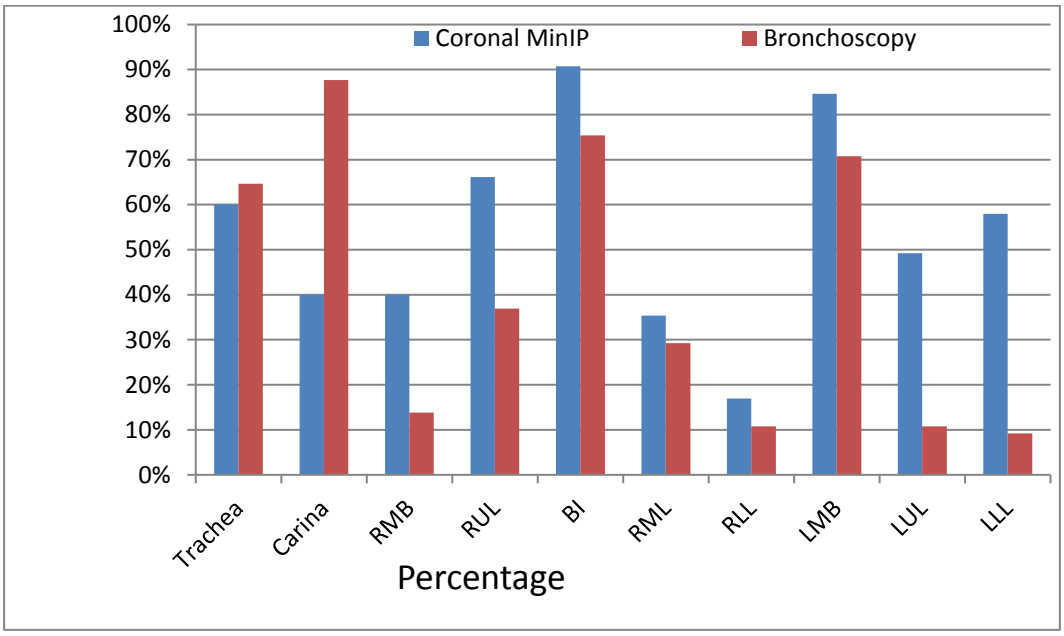

3.4.3. Comparison the degree of the airway stenosis of CT Min IP to FB

The detailed grading of the airways is summarised in tables 3.5, and 3.6 for both CT MinIP and FB respectively. Comparison of CT MinIP and FB with regard to severity of stenosis according to site and overall is summarised in table 3.8 and figure 3.4 - the commonest grade of the airway stenosis detected by the coronal CT Min IP reconstruction was grade 2 (17.5%) followed by grade 1 (16.6%), while the commonest grade found on FB was grade 1 (27.55%) followed by grade 2 (5.38%).

Table 3.8. Comparing the degree of airway stenosis on CT Min IP to FB

N= 650	Grade 1 >0-50%	Grade 2 51-75%	Grade 3a 76-99%	Grade 3b 100%	Total affected sites
Total Min IP	108 (16.6%)	114 (17.4%)	58 (9%)	72 (11%)	352 (54.2%)
Total FB	179 (27.54%)	35 (5.38%)	34 (5.23%)	18 (2.78%)	266 (41%)

Figure 3.4: Graph comparing the degree of the airway stenosis on CT MinIP to FB

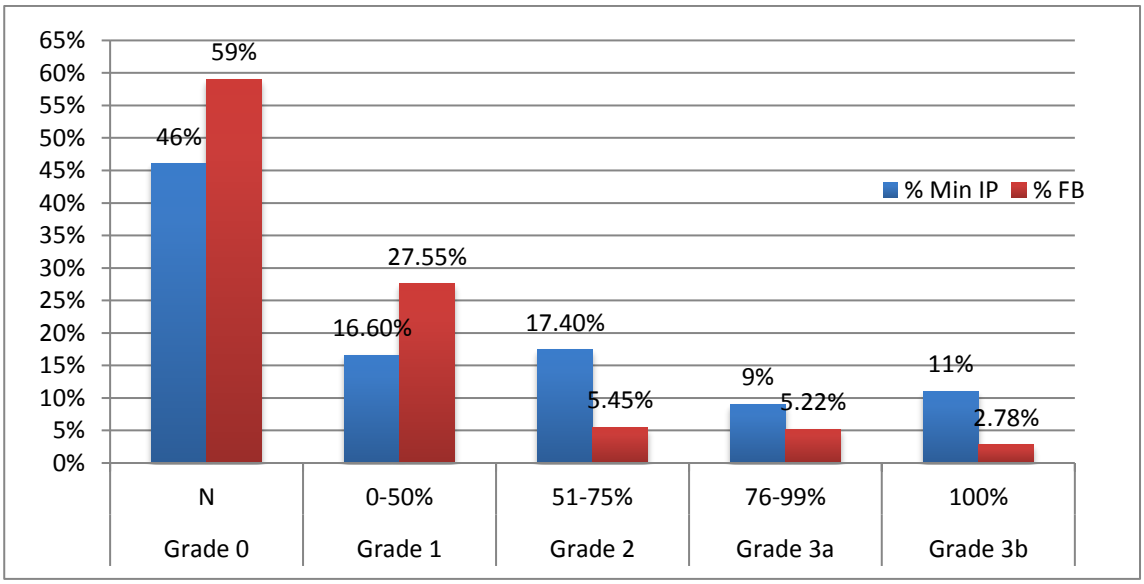

3.4.4. Comparing of the intraluminal lesions of CT MinIP to FB

There were 17 intraluminal lesions detected using FB and 23 intraluminal lesions reported using the coronal CT MinIP. The numbers of intraluminal lesions according to location for CT MinIP are summarised alongside those for FB in Table 3.9 and Figure 3.5.

Table 3.9. Comparison the intraluminal lesion between CT MinIP and FB

	Trachea	Carina	RMB	RUL	BI	RML	RLL	LMB	LUL	LLL	Total
CT MinIP	0	0	2	3	8	0	1	4	4	1	23
FB	0	0	3	1	6	0	2	3	1	1	17

Figure 3.5. A graph shows comparisons of intraluminal lesions detected by CT MinIP and FB

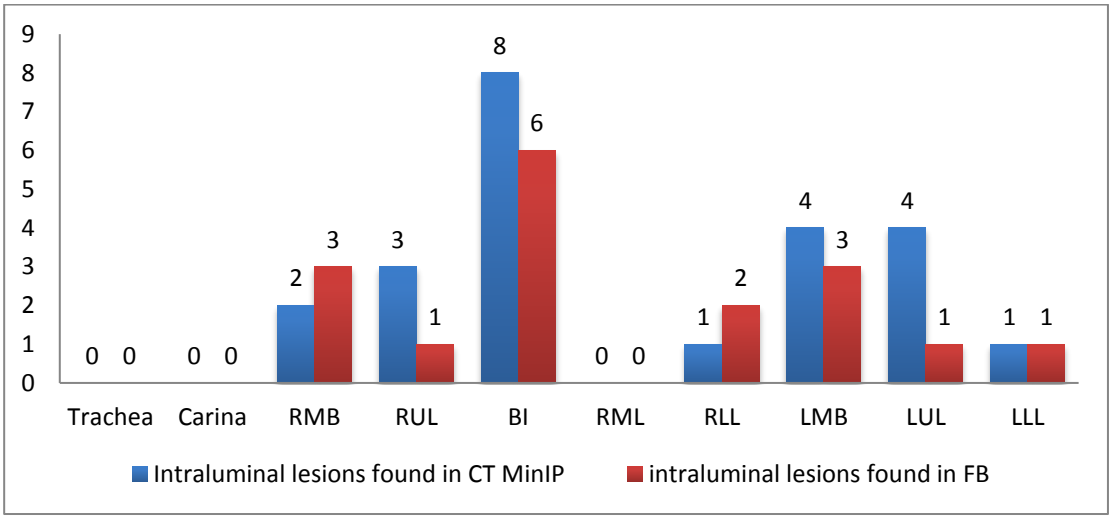

3.4.5. Sensitivity and specificity of CT MinIP and statistical comparison of coronal CT MinIP with FB for detection of airway stenosis

Sensitivity, specificity of MinIP (using the FB as the gold standard), are summarised in Table 3.10 and figure 3.6.

Table 3.10. Sensitivity, specificity of MinIP and comparison of CT MinIP against FB according to site

Site	Sensitivity of Coronal MinIP	Specificity of Coronal MinIP	Statistical significance P value
Trachea	64%	43%	0.5996
Carina	37%	38%	0.2497
RMB	78%	66%	0.0239
RUL	83%	44%	0.0314
BI	96%	25%	0.0286
RML	32%	63%	0.780
RLL	57%	89%	0.0127
LMB	89%	26%	0.1413
LUL	71%	53%	0.2576
LLL	67%	42%	1

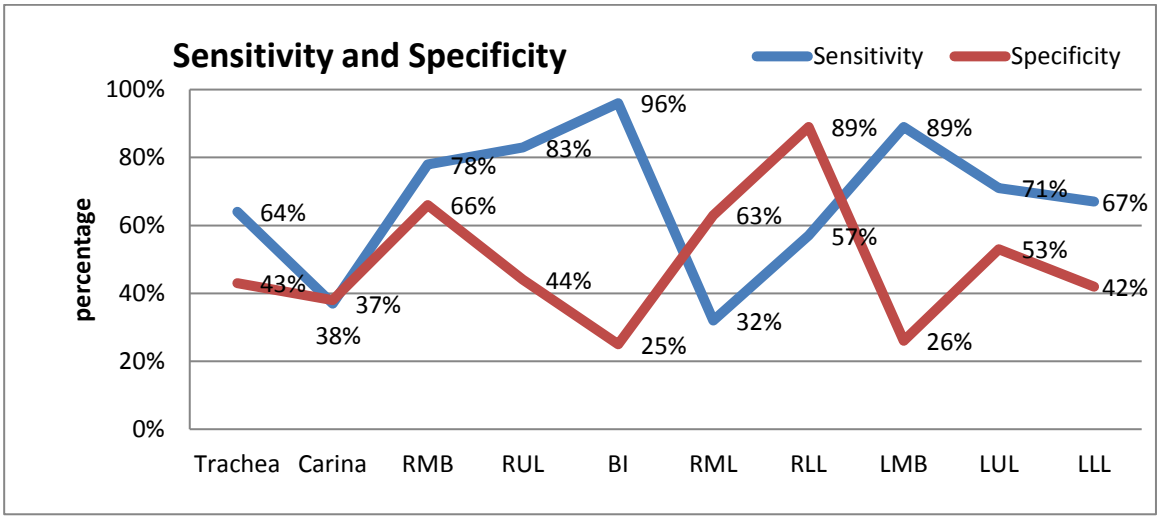

Figure 3.6. Sensitivity and specificity values of Coronal MinIP in detecting the stenosis for each site.

3.4.6. Agreement between coronal CT MinIP and FB regarding of stenosis and normal.

The agreement of a number of stenosed cases and normal cases between the coronal CT MinIP and FB summarized in the table 3.11 and because of this is a retrospective study; the levels and the sides of stenosis were not accounted in this agreement comparison.

Table 3.11. The agreement between the coronal CT MinIP and FB

	Stenosed MinIP only	Stenosed FB only	Normal agreement	Stenosis agreement	Total agreement N=65
Trachea	12	15	11	27	38 (58.46%)
Carina	5	36	3	21	24 (36.9%)
RMB	19	2	37	7	44 (67.7%)
RUL	23	4	18	20	38 (58.46%)
BI	12	2	4	47	51 (78.46%)
RML	17	13	29	6	35 (53.85%)
RLL	7	3	51	4	55 (84.6%)
LMB	14	5	5	41	46 (70.76%)
LUL	27	2	31	5	36 (55.4%)
LLL	33	1	26	5	31 (47.7%)
Total / N=650	169	83	215	183	398 (61.2%)

3.5. Comparison axial and coronal CT MinIP to FB in the detection of carinal stenosis.

Because of substantial difference between the coronal CT MinIP and FB results at the level of the carina, the primary investigator performed axial reconstructions at level of the carina and reviewed these. The results were compared against the FB and the coronal MinIP.

The final results of this comparison are summarised in Table 3.12.

Figure 3.7 shows examples comparing coronal and axial CT MinIP of the same patients.

Table 3.12. Comparison between coronal and axial MinIP and FB for the detection of carinal stenosis

	Coronal MinIP	Axial MinIP	FB	A1	A2	A3	Total Agreement
Carina	26	56	57	21	51	26	21

Key:
A1= Agreement between coronal MinIP and FB
A2= Agreement between axial MinIP and FB
A3= Agreement between axial MinIP and coronal MinIP
Total agreement = agreement on all three techniques

The table 3.13 shows the comparison between the cases with carinal stenosis on FB only (as in table 3.11) and the axial CT MinIP reconstruction of the same cases.

Table 3.13. Comparison of 36 cases with carinal stenosis on FB only with axial CT MinIP

	Number of stenosis
FB only*	36
Axial CT MinIP**	30
The agreement	30

Key: * FB only = the cases have stenosis on FB and not on Coronal CT MinIP as described in Table 3.11. ** The cases from the total 36 cases (FB only) that have stenosis on axial CT MinIP at the level of the carina.

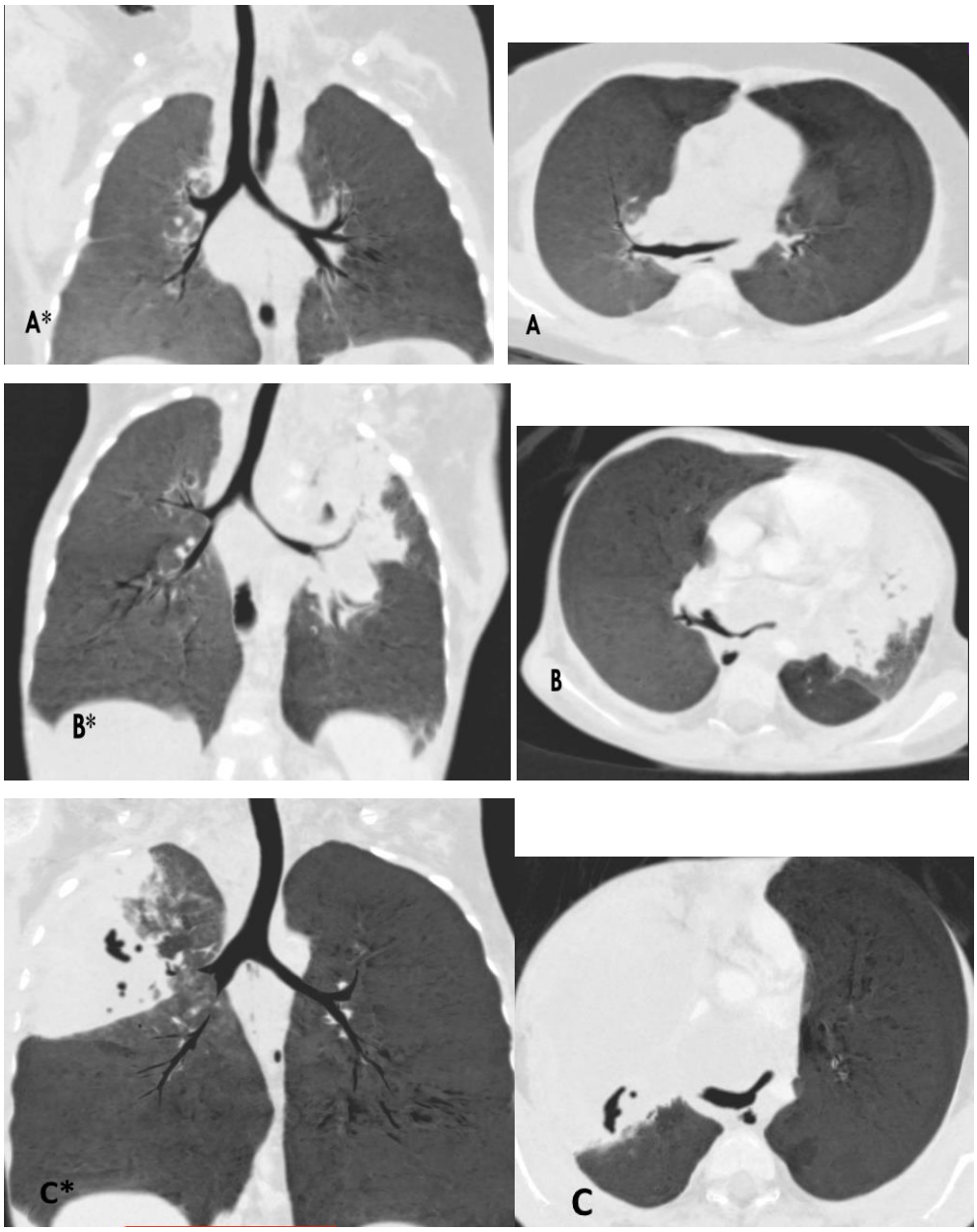

Figure 3.7. Three examples where the carina was considered normal on coronal CT MinIP but was determined to be abnormal on the axial CT MinIP

4.Discussion

4.1. Results in context and comparison of coronal CT MinIP reconstruction to FB

Airway obstruction or narrowing in LBTB may be extraluminal or intraluminal, where an extraluminal obstruction is typically caused by enlarged tuberculous lymph nodes. Although a single group of nodes could be involved, it is much more common for multiple nodal sites to be involved (25, 26). Intraluminal airway obstruction occurs by erosion of caseated lymph nodes into airways, or intraluminal inflammatory changes (25, 28, 30). The most common anatomical sites of airway compression by LBTB are the bronchus intermedius, and the left main bronchus (26, 29).

The most common sites of airway stenosis, as observed by coronal CT MinIP in this study, were the BI (91%), followed by the LMB (85%), the RUL (66%) and the trachea (60%). The results of the coronal CT MinIP compared well with other previous studies regarding airway stenosis in children with LBTB, which were observed with different modalities, including CT scans, 3D VR and CXR (15, 26, 29, 31). Table 4.1 compares the coronal CT MinIP findings of this study to the other three studies reporting airway stenosis due to LBTB in children, using different radiological diagnostic modalities.

Table 4.1 Comparisons of current results with three previous studies with regard to the most common airway stenosis observed, and the grading of the severity of the stenosis, as detected by CT scans.

	Du Plessis et al. 2009 (31)	Maydell et al. 2010 (29)	Lucas et al. 2012 (26)	Current study 2016
Number of patients	26	21	98	65
Median age of the patients	21 months	20 months	12 months	14 months
Modality of the study	(3D VR) MDCT	Multi-slice CT and CXR	MDCT	Coronal MinIP MDCT
Trachea affected	73% (19/26)	63% CXR	63% (62/98)	60% (39/65)
Bronchus intermedius affected	80.8% (21/26)	95% CT scan 90% CXR	74.5% (73/98)	91% (59/65)
Left main bronchus affected	92% (24/26)	81% CT scan 90% CXR	64.3% (63/98)	85% (55/65)
Right main bronchus affected	65.3% (17/26)	67% CT scan 57% CXR	20.4% (20/98)	40% (26/65)
Carina affected	57.7% (15/26)	Not stated	Not stated	40% (26/65)
Grade 1 (0-50%) stenosis	Most common	Not stated	Mild (0–33%) = 117	16.6% (108/650)
Grade 2 (51-75%) stenosis	Second most common	Not stated	Moderate (34–66%) = 82	17.4% (114/650)

Two-dimensional images like those produced using CT MinIP supply accurate measurements of diameter and craniocaudal length of airway stenoses, and provide complementary information about the airway stenosis and any tracheobronchial tree abnormalities when it is used in combination with three-dimensional (3D) CT images (41, 42). In this study, the standardised coronal CT MinIP images provided measurements of the length and the diameter of the airways at the level, above and below the stenotic sites, giving the CT MinIP an important advantage when compared to FB.

The coronal CT MinIP in this study provided more detailed information about the LBTB and any its complications compared to the FB. It delivered fundamental information about the airway stenosis, in terms of the degree of stenosis, the length of the stenosis, possible cause of the

stenosis in some cases (intraluminal lesion), and some obvious complication of the stenosis and LBTB (not evaluated in this research).

In this study, the total number of airway stenoses identified on CT MinIP was 352 out of 650 sites (54%), but only 266 out of 650 sites (41%) were identified by FB. Coronal CT MinIP successfully detected regions of airway stenosis in children with lymphobronchial TB with a sensitivity of up to 96% and specificity up to 89%.

The CT MinIP appears to be superior in detecting the small airway stenosis, and in those airways distal to areas of severe narrowing, compared to FB. Comparison between coronal CT MinIP and FB, regarding the detection of small airway stenoses distal to severe, and complete stenosis of the proximal major bronchial branches is summarised in Table 3.4.2. There were more stenoses detected by the coronal MinIP in small airways bilaterally compared to FB: 10% to 29% more on right side and 38% to 49.5% more on left side were detected by CT MinIP.

TB, and LBTBT in particular, can result in significant complications involving the lung parenchyma (25, 26). CT MinIP is useful in providing information about any lung parenchymal abnormalities over and above the detection of an airway stenosis (42, 43). Despite the limited imaging provided for review in this study, the single coronal CT MinIP slab still provided some additional parenchymal information in the form of consolidation, air trapping and cavitation as shown in Figure 4.1.

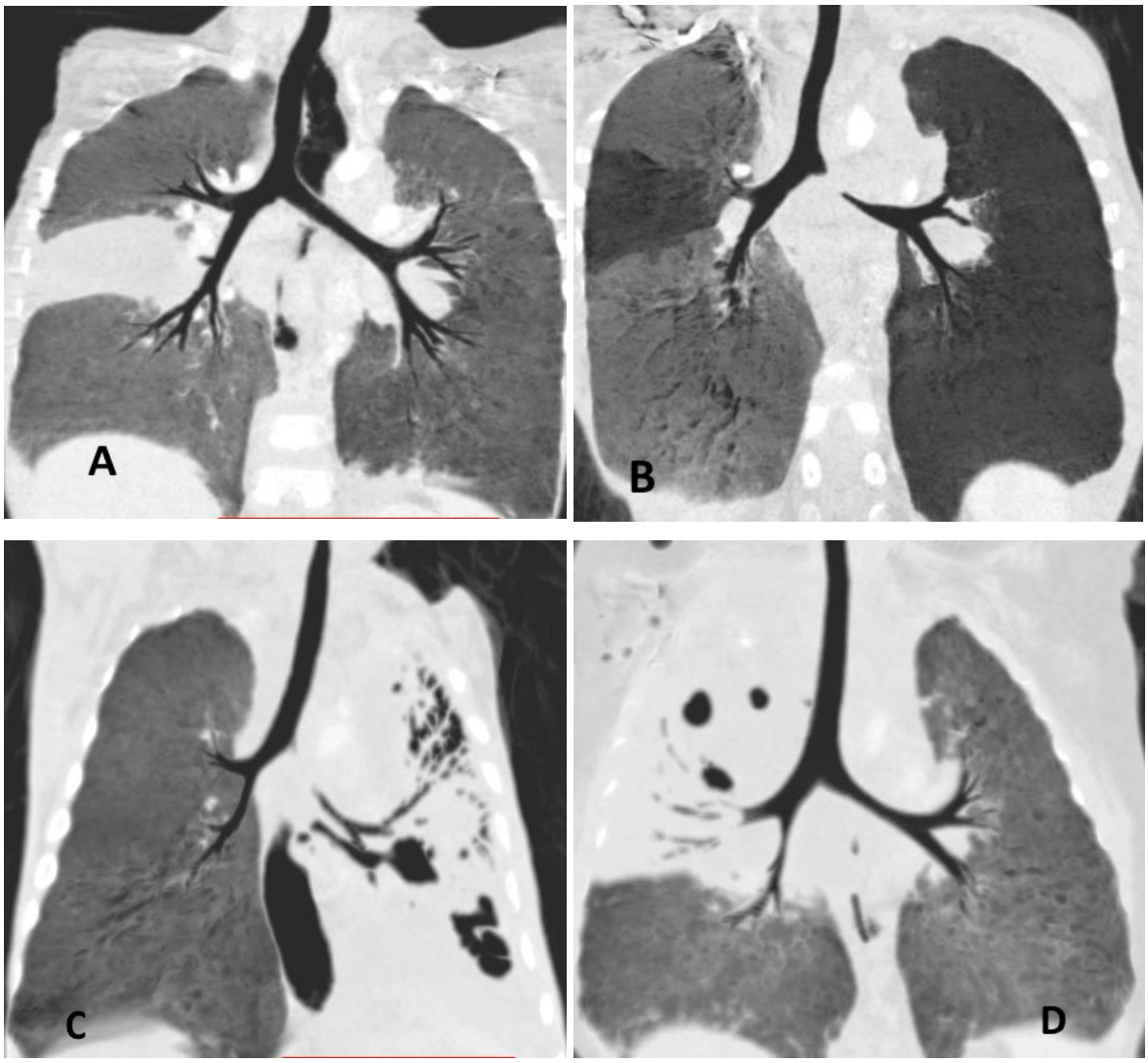

Figure 4.1: Shows consolidation of apical segment of the right lower lobe (A), right upper lobe and left lung air trapping (B), left lower cavitary lesions and left upper lobe consolidation (C), and right middle lobe consolidation with air bronchgram, right upper lobe dense consolidation (D).

FB showed superiority in detecting stenosis in the trachea (65%) and the carina (88%), compared to the coronal CT MinIP (60% in the trachea and 40% in the carina).
Carinal compression is more obvious on axial and sagittal MDCT and MPR (44, 45). In this study 30 of the 36 patients with stenosis recorded only on FB only (i.e. not detected on the coronal CT MinIP) had stenosis visible on axial MinIP - axial CT MinIP at the level of the carina showed close agreement with FB; (56/65, 86.2%) with the Axial CT MinIP, and (57/65, or 88%) with FB.

Sagittal CT scans and lateral CXR have been reported to be more sensitive and specific in recognising any lymphadenopathy around the carina which is attributed to the anatomical

locations of the lymph nodes in the retro-carinal, subcarinal and precarinal carina regions (44). Other MinIP or MPR reconstruction planes are recommended in combination with coronal CT MinIP for reporting the trachea and the major airways disease, based on the findings of this study. This is advisable to avoid missing compression or stenosis at the level of the carina.

The thickness of the slab in the single CT MinIP plays an important role in detecting and grading the stenosis (45). The slab thickness required in this study ranged from 10 to 20 mm for 62 of the cases (95.4%), and in only three cases (4.6%) was a slab thickness below 10 mm sufficient. The CT MinIP reconstruction can overestimate the degree of the stenosis (45, 46) and this was thought to be the case in our study- Grade 2 was the most common category of airway stenosis severity detected by the coronal CT MinIP (17.5%), followed by grade 1 (16.6%); while grade 1 (27.55%) was the most common category of airway stenosis severity on FB, followed by grade 2 (5.38%).

Flexible bronchoscopy has an important function in addition to diagnosis in that it can be used for treatment following airway involvement by LBTB or EBTB (33, 47). FB remains an invasive procedure that requires general anaesthesia (33), it carries significant costs, it has well described associated complications (34), and it can cause massive post-biopsy haemoptysis (48). Conversely, CT MinIP supplies acceptable detail for measuring the diameter and craniocaudal length of airway stenosis (41, 42), and it provides additional information on any lung parenchymal complications (42).

The coronal CT MinIP in this study revealed an acceptable correlation, when compared to FB, with reasonable agreement in detecting airway stenosis in children known to have LBTB. There was also good agreement between the techniques regarding the total normal and stenosed airways, which was best at the RLL (84.6%), followed by the BI (78.46%), the LMB (70.76%), and the RMB (67.7%).

The sensitivity of the coronal CT MinIP, using the FB as the gold-standard was considered very good in some branches of the airway— up to 96% in the BI, 89% in the LMB, 83% in the RUL, and 78% in the RMB. It was, however, very low in the RML (32%), and in the carina (37%). The specificity was, however, up to 89% in the RLL, 66% in the RMB, and 63% in the RML.

There are multiple advantages of coronal CT MinIP, which were highlighted in this study. It is not an invasive procedure, and it can add good value in determining endobronchial lesions, especially in the distal small bronchial trees, besides just detecting and grading airway stenosis, which gives an overall picture of the major airways and bronchial tree. CT MinIP also showed the ability to evaluate the small airways distal to the region with severe or complete stenosis, in addition to the capability of evaluating the lung parenchyma, and some complications due to the LBTB.

4.2. Standardised protocol for producing standardised coronal CT MinIP

In this study, a standardised protocol was developed for producing a coronal CT MinIP reconstruction image of the chest, for airway evaluation in children. This protocol can improve and add value during the diagnosis of different pathologies of children's airways, including congenital abnormalities, LBTB, endobronchial lesions, the presence of foreign bodies, and other causes of airway stenosis.

Reconstructing a single image from original MDCT data by a radiographers / technologist performing the study can take between two and five minutes; the reconstructed image can therefore be sent to with the source data for the radiologist to read. This provides the radiologist with the opportunity to gain an overview of the airways very quickly and to assess any airway abnormality including stenoses. The standardised image is also useful for demonstration and communication of anatomy and the pathology to the bronchoscopist and any surgeons involved in the management.

It is hoped that this study will provide the scientific support needed to change practice and stimulate the production of a standardised MinIP image of the airways for improving the diagnosis of airway abnormalities in children; furthermore it is hoped that the technique will assist physicians and surgeons in planning any invasive procedures. The radiologist is encouraged continue to use the source CT scan images, which will answer more questions about the airways, the parenchyma, and the lymphoadenopathy.
In this study, a standardised protocol was developed using six parameters (Appendix D)

to allow radiographers to produce a single coronal CT MinIP image of the tracheobronchial tree in children routinely.

4.3. Limitations of this study

The researcher acknowledges a potential limitation of this study related to the fact that all the patients in this study were known to have LBTB and airway stenosis. The researcher recognises that knowledge of the presence of abnormalities on MDCT and FB could have introduced bias. However, the site of stenosis was not known and there are a number of possible sites for stenosis in each patient – a total of 10 possible sites per patient.

It should be emphasised that the readers evaluated the coronal CT MinIP images blinded to the CT and FB findings, and it is unlikely that the readers were influenced by any LBTB complications.

This was a retrospective study, and all CT scans were performed without ensuring good patient positioning or lack of motion artefacts. Because of these types of quality issues, 35% of the potential patients were excluded from this study.

Coronal CT MinIP has limitations for detecting airway compression or stenosis in specific planes; it is recommended that the source CT scan of the chest be viewed in combination with the coronal CT MinIP.

5. Conclusion

This study has proven that a standardised coronal CT MinIP reconstruction is useful in demonstrating airway stenosis in children with lymphobronchial TB, with sensitivity of up to 96% and specificity up to 89%. The most common sites of stenosis found by the coronal MinIP CT reconstruction were the BI (91%), followed by the LMB (85%), the RUL (66%), and the trachea (60%). The coronal CT MinIP had additional advantages over FB in that it allowed objective measurement of the diameter of the stenosis, measurement of the length of the stenosis as well as visualisation of the post-stenotic segments of the airways. CT MinIP was also able to provide information about lung parenchymal abnormalities.

Standardised coronal MinIP reconstructions are easily performed, as described in our paper, and should be provided with each set of cross sectional MDCT images in children with LBTB. This one single image can provide easily appreciable and useful airway information and additional information not available from FB.

6. References

(1) Lawn SD, Zumla AI. 2011. Tuberculosis. *Lancet*, 378(9785):57-72.

(2) Perez-Velez CM, Marais BJ. 2012. Tuberculosis in children. *N Engl J Med*, 367(4):348-61.

(3) Kim WS, Choi JI, Cheon JE*, et al.* 2006. Pulmonary tuberculosis in infants: radiographic and CT findings. *AJR American journal of roentgenology*, 187(4):1024-33.

(4) Gray DM, Zar H, Cotton M. 2009. Impact of tuberculosis preventive therapy on tuberculosis and mortality in HIV-infected children. *Cochrane Database Syst Rev*, (1):CD006418.

(5) Rekha B, Swaminathan S. 2007. Childhood tuberculosis - global epidemiology and the impact of HIV. *Paediatr Respir Rev*, 8(2):99-106.

(6) WHO. 2013. GLobal Tuberculosis Report 2012. Available: http://www.who.int/tb/publications/global_report/en/ [Accessed on 3/10/2013].

(7) Mandalakas AM, Starke JR. 2005. Current concepts of childhood tuberculosis. *Seminars in pediatric infectious diseases*, 16(2):93-104.

(8) Starke JR. 2000. Diagnosis of tuberculosis in children. *The Pediatric infectious disease journal*, 19(11):1095-6.

(9) Kim WS, Moon WK, Kim IO*, et al.* 1997. Pulmonary tuberculosis in children: evaluation with CT. *AJR American journal of roentgenology*, 168(4):1005-9.

(10) Martinson NA, Moultrie H, van Niekerk R*, et al.* 2009. HAART and risk of tuberculosis in HIV-infected South African children: a multi-site retrospective cohort. *The international journal of tuberculosis and lung disease : the official*

journal of the International Union against Tuberculosis and Lung Disease, 13(7):862-7.

(11) Walters E, Cotton MF, Rabie H*, et al.* 2008. Clinical presentation and outcome of tuberculosis in human immunodeficiency virus infected children on anti-retroviral therapy. *BMC pediatrics*, 8:1.

(12) Lalvani A, Pareek M. 2010. Interferon gamma release assays: principles and practice. *Enfermedades infecciosas y microbiologia clinica*, 28(4):245-52.

(13) Sekadde MP, Wobudeya E, Joloba ML*, et al.* 2013. Evaluation of the Xpert MTB/RIF test for the diagnosis of childhood pulmonary tuberculosis in Uganda: a cross-sectional diagnostic study. *BMC infectious diseases*, 13:133.

(14) Nicol MP, Workman L, Isaacs W*, et al.* 2011. Accuracy of the Xpert MTB/RIF test for the diagnosis of pulmonary tuberculosis in children admitted to hospital in Cape Town, South Africa: a descriptive study. *The Lancet infectious diseases*, 11(11):819-24.

(15) Andronikou S, Joseph E, Lucas S*, et al.* 2004. CT scanning for the detection of tuberculous mediastinal and hilar lymphadenopathy in children. *Pediatric radiology*, 34(3):232-6.

(16) Andronikou S, Brauer B, Galpin J*, et al.* 2005. Interobserver variability in the detection of mediastinal and hilar lymph nodes on CT in children with suspected pulmonary tuberculosis. *Pediatric radiology*, 35(4):425-8.

(17) Arlaud K, Gorincour G, Bouvenot J*, et al.* 2010. Could CT scan avoid unnecessary flexible bronchoscopy in children with active pulmonary tuberculosis? A retrospective study. *Arch Dis Child*, 95(2):125-9.

(18) Garrido JB, Alias Hernandez I, Bonillo Perales A*, et al.* 2012. Usefulness of thoracic CT to diagnose tuberculosis disease in patients younger than 4 years of age. *Pediatric pulmonology*, 47(9):895-902.

(19) Yikilmaz A, Koc A, Coskun A*, et al.* 2011. Evaluation of pneumonia in children: comparison of MRI with fast imaging sequences at 1.5T with chest radiographs. *Acta Radiol*, 52(8):914-9.

(20) Gorkem SB, Coskun A, Yikilmaz A*, et al.* 2013. Evaluation of Pediatric Thoracic Disorders: Comparison of Unenhanced Fast-Imaging-Sequence 1.5-T MRI and Contrast-Enhanced MDCT. *AJR American journal of roentgenology*, 200(6):1352-7.

(21) Andronikou S, Wieselthaler N. 2004. Modern imaging of tuberculosis in children: thoracic, central nervous system and abdominal tuberculosis. *Pediatric radiology*, 34(11):861-75.

(22) Buxi TB, Sud S, Vohra R. 2002. CT and MRI in the diagnosis of tuberculosis. *Indian J Pediatr*, 69(11):965-72.

(23) Peprah KO, Andronikou S, Goussard P. 2012. Characteristic magnetic resonance imaging low T2 signal intensity of necrotic lung parenchyma in children with pulmonary tuberculosis. *Journal of thoracic imaging*, 27(3):171-4.

(24) Theart AC, Marais BJ, Gie RP*, et al.* 2005. Criteria used for the diagnosis of childhood tuberculosis at primary health care level in a high-burden, urban setting. *The international journal of tuberculosis and lung disease : the official journal of the International Union against Tuberculosis and Lung Disease*, 9(11):1210-4.

(25) Goussard P, Gie R. 2007. Airway involvement in pulmonary tuberculosis. *Paediatr Respir Rev*, 8(2):118-23.

(26) Lucas S, Andronikou S, Goussard P*, et al.* 2012. CT features of lymphobronchial tuberculosis in children, including complications and associated abnormalities. *Pediatric radiology*, 42(8):923-31.

(27) Tetikkurt C. 2008. Current perspectives on endobronchial tuberculosis. *Pneumon*, 21(3):239-45.

(28) Kreisel D, Arora N, Weisenberg SA*, et al.* 2007. Tuberculosis presenting as an endobronchial mass. *The Journal of thoracic and cardiovascular surgery*, 133(2):582-4.

(29) Maydell A, Goussard P, Andronikou S*, et al.* 2010. Radiological changes post-lymph node enucleation for airway obstruction in children with pulmonary tuberculosis. *European journal of cardio-thoracic surgery : official journal of the European Association for Cardio-thoracic Surgery*, 38(4):478-83.

(30) Prada Arias M, Jardon Bahia JA, Rodriguez Barca P*, et al.* 2006. Endobronchial tuberculous granuloma in children. *Eur J Pediatr Surg*, 16(4):265-8.

(31) du Plessis J, Goussard P, Andronikou S*, et al.* 2009. Comparing three-dimensional volume-rendered CT images with fibreoptic tracheobronchoscopy in the evaluation of airway compression caused by tuberculous lymphadenopathy in children. *Pediatric radiology*, 39(7):694-702.

(32) Nicolai T. 2001. Pediatric bronchoscopy. *Pediatric pulmonology*, 31(2):150-64.

(33) Goussard P, Gie RP, Kling S*, et al.* 2013. Bronchoscopic assessment of airway involvement in children presenting with clinically significant airway obstruction due to tuberculosis. *Pediatric pulmonology*, 48(10):1000-7.

(34) Midulla F, de Blic J, Barbato A*, et al.* 2003. Flexible endoscopy of paediatric airways. *Eur Respir J*, 22(4):698-708.

(35) Papagiannopoulos KA, Linegar AG, Harris DG*, et al.* 1999. Surgical management of airway obstruction in primary tuberculosis in children. *The Annals of thoracic surgery*, 68(4):1182-6.

(36) Lucas S, Andronikou S, Goussard P*, et al.* 2013. Tuberculous lymphadenopathy is not only obstructive but also inflammatory--it can erode anything it touches. Reply to Marchiori et al. *Pediatric radiology*, 43(2):254-5.

(37) Stansberry SD. 1990. Tuberculosis in infants and children. *Journal of thoracic imaging*, 5(2):17-27.

(38) Perandini S, Faccioli N, Zaccarella A*, et al.* 2010. The diagnostic contribution of CT volumetric rendering techniques in routine practice. *The Indian journal of radiology & imaging*, 20(2):92-7.

(39) Kirchgeorg MA, Prokop M. 1998. Increasing spiral CT benefits with postprocessing applications. *Eur J Radiol*, 28(1):39-54.

(40) Andronikou S, Irving B, Hlabangana LT*, et al.* 2013. Technical developments in postprocessing of paediatric airway imaging. *Pediatric radiology*, 43(3):269-84.

(41) Boiselle PM, Reynolds KF, Ernst A. 2002. Multiplanar and three-dimensional imaging of the central airways with multidetector CT. *AJR American journal of roentgenology*, 179(2):301-8.

(42) Lee KS, Boiselle PM. 2010. Update on multidetector computed tomography imaging of the airways. *Journal of thoracic imaging*, 25(2):112-24.

(43) Lee EY, Zucker EJ, Restrepo R*, et al.* 2013. Advanced large airway CT imaging in children: evolution from axial to 4-D assessment. *Pediatric radiology*, 43(3):285-97.

(44) Andronikou SVdM, DJ.; Goussard, P.; Tomazos, N. 2012. Usefulness of lateral radiographs for detecting tuberculous lymphadenopathy in children – confirmation using sagittal CT reconstruction with multiplanar cross-referencing. *sajr*, Vol 16(3):5.

(45) Sundarakumar DK, Bhalla AS, Sharma R*, et al.* 2011. Multidetector CT evaluation of central airways stenoses: Comparison of virtual bronchoscopy, minimal-intensity projection, and multiplanar reformatted images. *The Indian journal of radiology & imaging*, 21(3):191-4.

(46) Wang R, Liang C, Huang M*, et al.* 2012. Multidetector CT diagnosis of tracheobronchial stenosis associated with congenital heart diseases in pediatric patients. *RANZCR-AOCR 2012*, R-0055:1-17.

(47) Cakir E, Uyan ZS, Oktem S*, et al.* 2008. Flexible bronchoscopy for diagnosis and follow up of childhood endobronchial tuberculosis. *The Pediatric infectious disease journal*, 27(9):783-7.

(48) Kang ES, Choi YR, Lee KM*, et al.* 2014. Massive hemoptysis after a bronchoscopic biopsy in patients with endobronchial tuberculosis. *Chinese Medical Journal*, 127(21):3837-2.

Appendix A. Ethics clearance certificate

M130664

R14/49 Dr Ahmed O Krim et al

HUMAN RESEARCH ETHICS COMMITTEE (MEDICAL)

CLEARANCE CERTIFICATE NO. M130664

NAME: (Principal Investigator)	Dr Ahmed O Krim et al
DEPARTMENT:	Radiology Department of Radiation Science
PROJECT TITLE:	Comparison of Coronal Minimum Intensity Projection Computed Tomography Images with Fibre Optic Flexible Bronchoscopy for Airway Compression in Children with Lymphoronchial Tuberculosis
DATE CONSIDERED:	28/06/2013
DECISION:	Approved unconditionally
CONDITIONS:	
SUPERVISOR:	Dr S Lucas
APPROVED BY:	Professor PE Cleaton-Jones, Chairperson, HREC (Medical)

DATE OF APPROVAL: 28/06/2013

This clearance certificate is valid for 5 years from date of approval. Extension may be applied for.

DECLARATION OF INVESTIGATORS

To be completed in duplicate and **ONE COPY** returned to the Secretary in Room 10004, 10th floor, Senate House, University.

I/we fully understand the conditions under which I am/we are authorized to carry out the above-mentioned research and I/we undertake to ensure compliance with these conditions. Should any departure be contemplated, from the research protocol as approved, I/we undertake to resubmit the application to the Committee. **I agree to submit a yearly progress report**.

Principal Investigator Signature Date

PLEASE QUOTE THE PROTOCOL NUMBER IN ALL ENQUIRIES

Appendix B. Working sheet for identifying the site of stenosis and degree of compression on coronal MIP CT

Study number	
Age	
Gender	

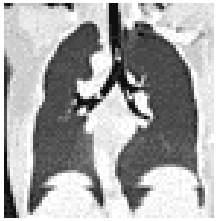

Grading of obstruction	
0 = No obstruction	0%
1 = Mild obstruction	1-50%
2 = Moderate obstruction	51-75%
3 a = Severe obstruction	76-99%
3 b = Complete obstruction	100%

	Stenosed?	Airway measurements			Calculations	
Site	Y/N	Normal above stenosis N	Stenosis minimum S	Stenosis Length	Percent (%) (S/N) X 100	Grade
Trachea						
Carina						
RMB						
RUL						
BI						
RML						
RLL						
LMB						
LUL						
LLL						

Appendix C. Working sheet for identifying the site of stenosis and degree of compression on bronchoscopy

Study number	
Age	

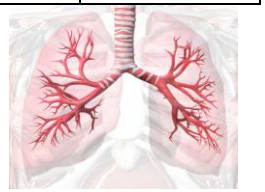

Grading of obstruction	
0 = No obstruction	0%
1 = Mild obstruction	1-50%
2 = Moderate obstruction	51-75%
3 a = Severe obstruction	76-99%
3 b = Complete obstruction	100%

Site	Stenosed? Y/N	Normal above stenosis	Stenosis Length if Available	Percent (%) Of the stenosis	Grade
Trachea					
Carina					
RMB					
RUL					
BI					
RML					
RLL					
LMB					
LUL					

Appendix D. Standardised protocol for producing standardised Coronal CT MinIP

➢ Open the CT scan serial in the MPR application, whereby, the trachea on sagittal plane must be peripendicular to the carina on the axial plane, using the vertical and transverse axis, with the midpoint at the Level of the carina.	
➢ The correction of the orintation of the coronal view is planned by angling the transverse axis along the carina, and by keeping the vertical axis along the trachea on the coronal plane view.	
➢ Change the soft tissue window to the lung window and select MinIP reconstruction	
➢ Select the acceptable thickness of MinIP reconstruction ranged between 5 to 20 mm; the slab thickness must give full visualization of trachea and major bronchi on the coronal image	
➢ Save the single image, annotate it with a number or name; centralize and zoom the image	
➢ Send the single image post reconstruction to the reporting station for the radiologist to read	

Appendix E: Note on referencing style

Please note that the referencing in this thesis is a modification of the Vancouver Referencing style, done according to the Faculty of Health Sciences Style Guide as set out by the Wits Health Sciences Library.

The information on this WHSL Vancouver Citation Style Guide for Theses, Dissertations and Research Reports is available from http://libguides.wits.ac.za/whsl-vancouver updated on 30 January 2017.